ISBN: 978-3-95450-191-5 doi:10.18429/JACoW-SRF2017-THPB042

# FIELD-DEPENDENCE OF THE SENSITIVITY TO TRAPPED FLUX IN $Nb_3Sn$*

D.L. Hall†, M.Liepe, R.D. Porter, D.B. Liarte, J.P. Sethna
Cornell Laboratory for Accelerator-Based Sciences and Education (CLASSE),
Ithaca, NY 14853, USA

*Abstract*

The amount of residual resistance gained per unit of trapped flux – referred to as the trapped flux sensitivity – in $Nb_3Sn$ cavities has been found to be a function of the amplitude of the RF field. This behaviour is consistent with a scenario in which the trapped vortex dynamics are described by collective weak pinning. A model has been developed to describe this, and results in the observed linear dependence of trapped flux sensitivity with RF field. The model is used to discuss cavity preparation methods that might suppress this dependence, which would reduce the trapped flux requirements necessary to operate an $Nb_3Sn$ cavity at simultaneous high quality factors and accelerating gradients.

## INTRODUCTION

Niobium cavities coated with a layer of $Nb_3Sn$ are a promising high-efficiency alternative to more conventional niobium for SRF applications [1–5]. In particular, the lower BCS resistance of $Nb_3Sn$ allows operation of 1.3 GHz cavities at a bath temperature of 4.2 K, permitting the use of cryo-coolers or liquid helium without active pumping. To allow this to happen, however, the other components of the surface resistance, vis-à-vis residual resistance, must be minimised.

The greatest contributor to the surface resistance from source other than BCS are contributions from trapped magnetic flux. The losses from trapped flux are linearly proportional to the amount of flux trapped, and are quantified by the sensitivity to trapped flux, in nΩ of residual gained per mG of flux trapped. Results given here show that the sensitivity to trapped flux in $Nb_3Sn$ films on niobium possess a noticeable dependence on the applied RF field, in a similar fashion seen to niobium films sputtered onto copper [6]. In this paper we demonstrate that this behaviour is consistent with a weak collective flux pinning scenario, in which a loss term from the presence of many weak pinning sites is introduced into the flux vortex equations of motion.

## EXPERIMENTAL METHOD

An ILC-style single-cell 1.3 GHz cavity, niobium coated with $Nb_3Sn$, was utilised for this experiment. The cavity was tested in a vertical cryostat, using an experimental arrangement described by the diagram in Fig. 1. A Helmholtz coiled mounted over the cavity allowed the application of a near-constant magnetic field along the beam axis of the cavity, while a heater located at the base of the cryostat allowed the application of a thermal gradient across the cavity during the cool-down through $T_c$. The latter is necessary for the generation of thermoelectric currents from the metal bilayer interface of Nb/$Nb_3Sn$, which will result in the generation of a thermally-induced magnetic field. This measurement was used to demonstrate that the application of a thermal gradient during cool-down is equivalent to the application of an external magnetic field.

## RESULTS

The equivalence of a thermal gradient to an externally applied magnetic field during cool-down is demonstrated in Fig. 2. In both cases, a linear increase in the $\Delta T$ across the cavity (measured in K/m) or an equivalent increase in the external magnetic field results in an increases in the residual resistance. This linear dependence allows us to quote an equivalence factor between the two sources for this cavity, which was found to be (6.2 ± 0.3) mG/(K/m).

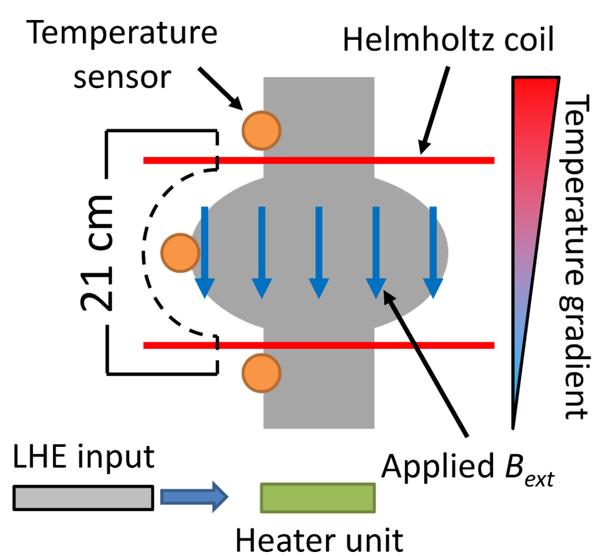


Figure 1: Diagram illustrating the experimental setup of the single-cell cavity. Liquid helium is introduced in a control fashion at the base of the cryostat, which, in the absence of power from the heater unit, allows cooling in an almost-uniform gradient. The Helmholtz coil allows the application of an external magnetic field, whilst the use of the heater develops a temperature gradient across the cavity, measured by the Cernox sensors mounted on the equator and irises.

* This work was primarily supported by U.S. DOE award DE-SC0008431. This work was supported in part by the U.S. National Science Foundation under Award PHY-1549132, the Center for Bright Beams.
† dlh269@cornell.edu

ISBN: 978-3-95450-191-5 doi:10.18429/JACoW-SRF2017-THPB042

A linear fit of the trapped flux as a function of the trapped magnetic field (and, through use of the equivalence factor stated previously, the $\Delta T$ as a function of the same) determines the sensitivity to trapped flux. By performing the measurement at different RF fields, the sensitivity as a function of the applied RF field can be determined. This measurement is shown in Fig. 3. As can be seen, the sensitivity follows a linear trend between the measured values of 5-45 mT, described by the the relation

$$\frac{dR}{dB_{\text{trapped}}} = R^0_{fl} + R^1_{fl} \times B_{rf} \,, \tag{1}$$

where $B_{rf}$ is the peak applied RF magnetic field in the cavity. Our data give a slope of $R^1_{fl} = (21 \pm 1)$pΩ/mG/mT and a y-intercept of $R^0_{fl} = (0.47 \pm 0.02)$nΩ/mG.

This linear form for the flux component of residual resistance has previously been strongly observed in niobium sputtered on copper substrates [6], as well as, less strongly, in bulk niobium [7, 8]. Measurements of $R^0_{fl}$ and $R^1_{fl}$ for niobium-based cavities from literature are compared to the result given in this paper in Fig. 4. As can be seen, the slope in bulk niobium cavities is comparatively mild, although the addition of nitrogen as a dopant appears to cause a mild increase in $R^1_{fl}$ alongside a strong increase in $R^0_{fl}$. However, in niobium sputtered onto copper, the slope $R^1_{fl}$ is considerably stronger, in stark contrast to having a far lower value of the offset $R^0_{fl}$. In the literature cited for niobium sputtered on copper [6], the slope and offset were found to be a function of the sputtering gas mixture. If the linear dependence of the sensitivity in $Nb_3Sn$ can be understood from a theoretical perspective, it may be possible to deduce an alteration in the production method that can similarly affect the values of $R^{0,1}_{fl}$, with the intent of minimising them.

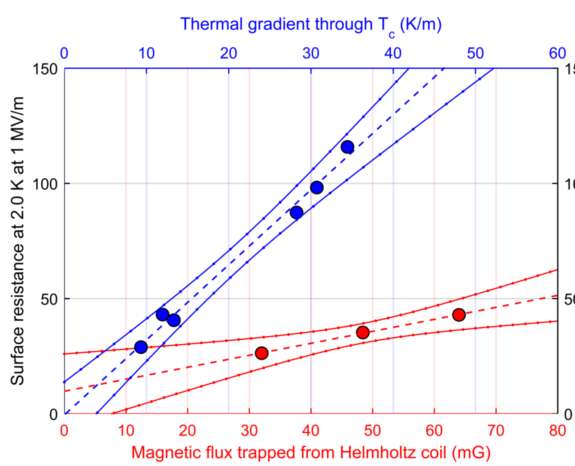


Figure 2: Measurements of the increase in residual resistance as a function of the applied thermal gradient (in blue) and trapped ambient magnetic field (in red) during the cool-down through $T_c$.

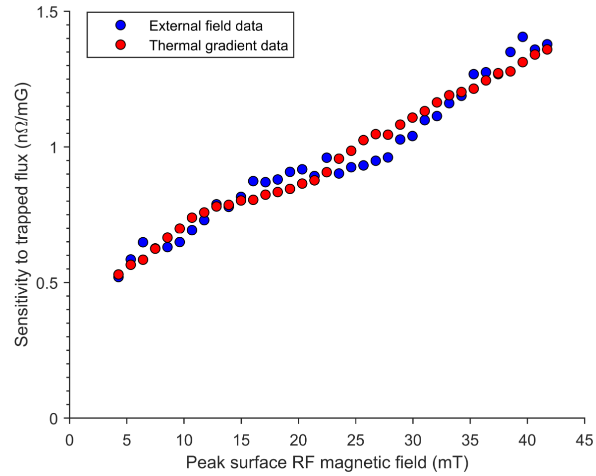


Figure 3: A measurement of the sensitivity to trapped flux, using data from both Helmholtz coil (blue) and thermal gradient (red) cool-downs, as a function of the applied RF magnetic field in the cavity.

## WEAK COLLECTIVE FLUX PINNING MODEL

In this scenario, the vortex line is displaced from its neutral position by the application of the RF field, whose strength overcomes the weak pinning centres near the RF surface. The scenario is depicted in Fig. 5. The force applied by the Lorentz force is propagated along the vortex line by the elastic line tension, which causes the oscillation to extend further into the bulk, out of the influence of the RF field. Deeper into the bulk, the force transmitted by the line tension is weakened by the elastic nature of the vortex line and so is less able to overcome the pinning force, until deep enough into the bulk the flux line is pinned in the same manner considered in a strong pinning scenario, unaffected by the actions of the Rf field at the surface.

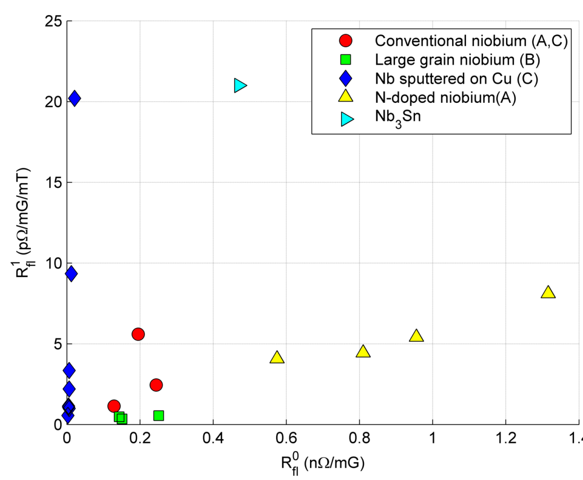


Figure 4: Values from literature for the offset $R^0_{fl}$ and slope $R^1_{fl}$ from Equation 1. The legend indicates the source of the data: (A) [7], (B) [8], and (C) [6].

ISBN: 978-3-95450-191-5 doi:10.18429/JACoW-SRF2017-THPB042


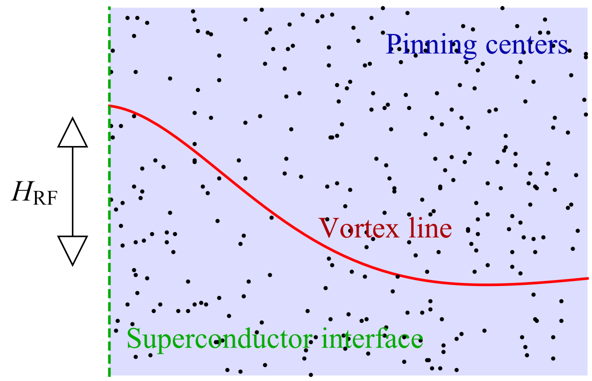

Figure 5: A representation of the weak collective flux pinning model. A vortex line, oscillating under the influence of the RF field, dissipates power into the superconductor due to the force imposed by a high density of weak pinning sites.

As the vortex line reaches its peak displacement under the RF field, and the Lorentz force starts decreasing, the same pinning centres also oppose the restoration of the vortex line to its original shape. This results in a shape being drawn out by the vortex line in a manner seen in Fig. 6, with two parabolas of opposite curvatures describing the shape of the vortex as it changes direction of travel under the influence of the RF field.

It is this manner of motion that gives rise to a sensitivity dependent upon the magnitude of the RF field, $B_{rf}$. Solving the Bardeen-Stephen equation of motion [9], neglecting the viscous, effective mass and Magnus terms while maintaining the contribution from the Lorentz, elastic, and pinning forces, results in a sensitivity given by

$$\frac{R_0}{B_{\text{trapped}}} = AB_{rf}, \tag{2}$$

where

$$A = \frac{4}{3}\frac{f\lambda^2\mu_0}{{B_c}^2\xi}\left(\frac{j_o}{j_c}\right)^{3/2}, \tag{3}$$

with $f$ being the RF frequency, $\lambda$ the superconducting penetration depth, $B_c$ the thermodynamic critical field, and $\xi$ the superconducting coherence length. The terms $j_o$ and $j_c$ are the de-pairing current (at which point the Cooper pairs are broken) and de-pinning current (at which point the flux line is de-pinned), respectively. Using Ginzburg-Landau theory, the former can be written as

$$j_o = \frac{4}{3\sqrt{6}\mu_0}\frac{B_c}{\lambda}. \tag{4}$$

Although this analytical solution does not consider the impact of viscous forces (which are not negligible), it demonstrates that a linear dependence of the sensitivity to trapped flux is consistent with a weak collective flux pinning scenario. Efforts are currently underway to re-introduce the viscous term using numerical solutions, to allow direct comparison to experiment.

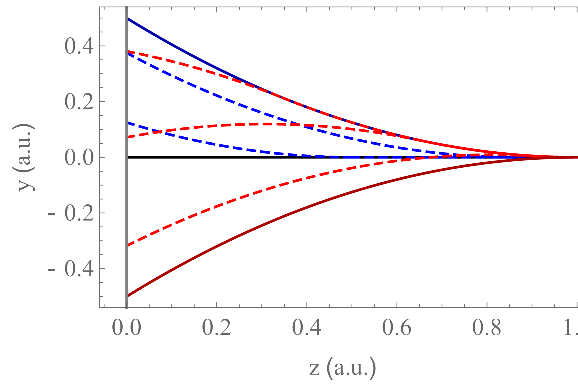

Figure 6: Motion of a flux line under the influence of the RF field in a weak collective flux pinning scenario. During the initial phase, the vortex line is displaced from neutral (blue) until it reaches the peak of its oscillation. As the Lorentz force starts decreasing and the vortex moves in the opposite direction (red), the impact of the weak pinning sites changes the sign of the curvature near the tip of the vortex.

## CONCLUSION

The sensitivity to trapped flux of $Nb_3Sn$ cavities has been shown to be a linear function of the applied RF field, a behaviour seen previously in cavities of niobium sputtered on copper. This linear increase with RF field has been shown to be consistent with a weak collective flux pinning scenario of trapped vortex motion. As it currently stands, this phenomenon places a constraint on the requirements for operating an $Nb_3Sn$ cavity in a cryomodule, specifically in terms of the amount of trapped flux that can be sustained before the additional losses from the residual resistance prohibit operation at target fields. From our data, it appears that a target of 100 mK/m of thermal gradient across the cavity, in 1-2 mG of ambient magnetic field, is sufficient to guarantee a quality factor of $> 10^{10}$ at 4.2 K and 16 MV/m in an ILC-style 1.3 GHz cavity. Although quite demanding, these operating parameters are not unreasonable, and have been obtained in contemporary cryomodules. However, given the distribution of values of $R_{fl}^{0,1}$ seen in literature, it appears that both a “cleaning” of the superconductor or the introduction of strong pinning sites could be successful in reducing the slope, through affecting the penetration depth $\lambda$ or the de-pinning current $j_c$.

## REFERENCES

[1] D. L. Hall, J. J. Kaufman, M. Liepe, R. D. Porter, and J. Sears, “First Results From New Single-Cell Nb3Sn Cavities Coated at Cornell University,” in *Proceedings of IPAC 2017*, Copenhagen, Denmark, [Online]. Available: https://doi.org/10.18429/JACoW-IPAC2017-MOOCA2, May 2017.

[2] S. Posen and D. L. Hall, “Nb3Sn superconducting radiofrequency cavities: fabrication, results, properties, and prospects,” *Superconductor Science and Technology*, vol. 30, no. 3, p. 33004, 2017. [Online]. Available: http://stacks.iop.org/0953-2048/30/i=3/a=033004

ISBN: 978-3-95450-191-5 doi:10.18429/JACoW-SRF2017-THPB042


[3] D. L. Hall, "Next generation Nb3Sn cavities: Current performance, limitations, and considerations for practical use," in *Presented at the Tesla Technology Collaboration meeting at CEA Saclay*, Paris, 2016.

[4] D. L. Hall, M. Liepe, and J. Maniscalco, "RF Measurements on High Performance Nb3Sn Cavities," in *Proceedings of IPAC 2016*, Busan, May 2016. [Online]. Available: https://doi.org/10.18429/JACoW-IPAC2016-WEPMR024, 2016.

[5] S. Posen, M. Liepe, and D. L. Hall, "Proof-of-principle demonstration of nb3sn superconducting radiofrequency cavities for high q0 applications," *Applied Physics Letters*, vol. 106, no. 8, p. 082601, 2015. [Online]. Available: http://dx.doi.org/10.1063/1.4913247

[6] C. Benvenuti, S. Calatroni, I. Campisi, P. Darriulat, C. Durand, M. Peck, R. Russo, and A.-M. Valente, "Magnetic Flux Trapping in Superconducting Niobium," in *Proceedings of SRF 1997*, Abano Terme, 1997.

[7] M. Martinello, M. Checcin, A. Grassellino, O. Melnychuk, S. Posen, A. Romanenko, and D. Sergatskov, "Trapped Flux Surface Resistance for Different Surface Treatments," in *Proceedings of SRF 2015*, Whistler, [Online]. Available: https://doi.org/10.18429/JACoW-SRF2015-MOPB015, 2015.

[8] G. Ciovati and A. Gurevich, "Measurement of RF losses due to Trapped Flux in a Large-Grain Niobium Cavity," in *Proceedings of SRF 2007*, Beijing, 2007.

[9] J. Bardeen and M. J. Stephen, "Theory of the motion of vortices in superconductors," *Phys. Rev.*, vol. 140, pp. A1197–A1207, Nov 1965. [Online]. Available: http://link.aps.org/doi/10.1103/PhysRev.140.A1197